European Journal of Medicinal Chemistry 65 (2013) 533–545

Contents lists available at SciVerse ScienceDirect

European Journal of Medicinal Chemistry

journal homepage: http://www.elsevier.com/locate/ejmech

Original article

New linezolid-like 1,2,4-oxadiazoles active against Gram-positive multiresistant pathogens

Cosimo G. Fortuna [a,*], Carmela Bonaccorso [a], Alessandra Bulbarelli [b], Gianluigi Caltabiano [c], Laura Rizzi [b], Laura Goracci [a], Giuseppe Musumarra [a], Andrea Pace [d,e,**], Antonio Palumbo Piccionello [d,e], Annalisa Guarcello [d,e], Paola Pierro [d,e], Clementina E.A. Cocuzza [f], Rosario Musumeci [f,***]

[a] Dipartimento di Scienze Chimiche, Università degli Studi di Catania, Viale Andrea Doria 6, I-95125 Catania, Italy
[b] Dipartimento di Scienze della Salute, Università di Milano-Bicocca, Via Cadore 48, I-20900 Monza, MB, Italy
[c] Laboratori de Medicina Computacional, Unitat de Bioestadística, Facultat de Medicina, Universitat Autònoma de Barcelona, 08193 Bellaterra, Spain
[d] Dipartimento di Scienze e Tecnologie Molecolari e Biomolecolari (STEMBIO), Sez. Chimica Organica "E. Paternò", Università degli Studi di Palermo, Viale delle Scienze Ed. 17 – Parco D'Orleans II, I-90128 Palermo, Italy
[e] Istituto EuroMediterraneo di Scienza e Tecnologia (IEMEST), Via Emerico Amari 123, I-90139 Palermo, Italy
[f] Dipartimento di Chirurgia e Medicina Interdisciplinare, Università di Milano-Bicocca, Via Cadore 48, I-20900 Monza, MB, Italy

ARTICLE INFO

Article history:
Received 26 August 2012
Received in revised form
25 February 2013
Accepted 31 March 2013
Available online 14 May 2013

Keywords:
Oxazolidinones
Linezolid
Drug design
Antimicrobial activity
Cell viability
Staphylococcus aureus

ABSTRACT

The synthesis and the *in vitro* antibacterial activity of novel linezolid-like oxadiazoles are reported. Replacement of the linezolid morpholine C-ring with 1,2,4-oxadiazole results in an antibacterial activity against *Staphylococcus aureus* both methicillin-susceptible and methicillin-resistant comparable or even superior to that of linezolid. While acetamidomethyl or thioacetoamidomethyl moieties in the C(5) side-chain are required, fluorination of the phenyl B ring exhibits a slight effect on an antibacterial activity but its presence seems to reduce the compounds cytotoxicity. Molecular modeling performed using two different approaches – FLAP and Amber software – shows that in the binding pose of the newly synthesized compounds as compared with the crystallographic pose of linezolid, the 1,2,4-oxadiazole moiety seems to perfectly mimic the function of the morpholinic ring, since the H-bond interaction with U2585 is retained.

1. Introduction

Use and misuse of antibacterial agents have resulted in the development of bacterial resistance to all antibiotics in clinical use irrespective of the chemical class or molecular target of the drug. Infections caused by multiresistant Gram-positive cocci, such as methicillin-resistant *Staphylococcus aureus* (MRSA), vancomycin-resistant enterococci (VRE) and penicillin-resistant *Streptococcus pneumoniae* (PNSSP), have emerged as major public health concern, both in hospital and community settings worldwide. The need for new antibiotics urged the Infectious Disease Society of America (IDSA) to issue the challenge to develop ten new antibiotics by 2020 [1].

Oxazolidinones are a class of antibacterial agents which displayed activity against a variety of Gram-positive pathogens and are highly potent against multidrug-resistant bacteria. In particular, oxazolidinones are used to treat skin and respiratory tract infections caused by *S. aureus* and streptococci strains, as well as being active against vancomycin-resistant *Enterococcus faecium* [2,3]. Linezolid (Fig. 1), the first oxazolidinone antibiotic approved for clinical use, has been shown to inhibit translation at the initiation phase of protein synthesis in bacteria by binding to the 50S ribosomal subunit [4]. Since 2001, however, linezolid resistance began to appear in *S. aureus* and *E. faecium* clinical isolates and the rate of resistance raised especially among enterococci and *Staphylococcus epidermidis* strains with its usage [5–8].

* Corresponding author. Tel.: +39 0957385010; fax: +39 095580138.
** Corresponding author. Dipartimento di Scienze e Tecnologie Molecolari e Biomolecolari (STEMBIO), Sez. Chimica Organica "E. Paternò", Università degli Studi di Palermo, Viale delle Scienze Ed. 17 – Parco D'Orleans II, I-90128 Palermo, Italy. Tel.: +39 09123897543; fax: +39 091596825.
*** Corresponding author. Tel.: +39 (0)264488103; fax: +39 (0)264488363.
E-mail addresses: cg.fortuna@unict.it (C.G. Fortuna), andrea.pace@unipa.it (A. Pace), rosario.musumeci@unimib.it (R. Musumeci).

0223-5234/$ – see front matter © 2013 Elsevier Masson SAS. All rights reserved.
http://dx.doi.org/10.1016/j.ejmech.2013.03.069

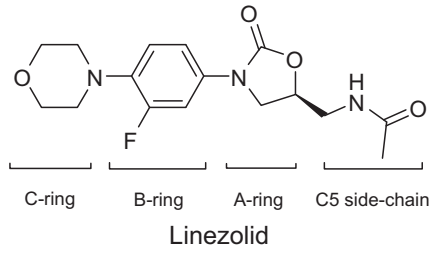

Fig. 1. Structure and portions nomenclature of linezolid.

A number of solutions to the problem of bacterial resistance are possible. Successful strategies include combination of existing antibacterial agents with other drugs as well as the development of improved diagnostic procedures that may lead to rapid identification of the causative pathogen and permit the use of antibacterial agents with a narrow spectrum of activity. Another strategy is the discovery of novel classes of antibacterial agents acting through new mechanisms of action. However, the most common approach, and still the most promising one, is the modification of existing classes of antibacterial agents to provide new analogs with improved activities.

In this context many researchers tried to modify the structure of linezolid to improve the antibacterial activity [9–14]. In order to rationalize the site of modifications, the structure of linezolid can formally be divided into four portions according to oxazolidinone antibacterials nomenclature [9]: i) the A-ring, consisting of the oxazolidinone central heterocycle; ii) the B-ring, consisting of a *N*-aryl moiety linked to the oxazolidinone nitrogen; iii) the C-ring, consisting of either a carbo- or heterocyclic-functional group, not necessarily aromatic; iv) the side-chain, consisting of any functional group linked to the oxazolidinone C(5) or in an isosteric position with respect to an A-ring of general type (Fig. 1).

Different types of modifications are reported in literature; the most common one regards the C-ring, while only few modifications were reported for the A-ring, and in some cases good activity was retained [15,16].

Our group previously reported that the replacement of the oxazolidinone (A-ring) with an isosteric 1,2,4-oxadiazole heteroaromatic ring resulted in a lack of activity [17]. Therefore, these compounds have been chosen as references for inactive linezolid-like compounds in a virtual screening approach.

Due to the lack of pharmacological targets, in previous studies [18] some of us already applied a Virtual Receptor Site (VRS) approach adopting a Molecular Interaction Field (MIF) approach using Grid Independent Descriptors (GRIND) calculated using the program Pentacle, which is based on the assumption that the process of ligand–receptor interaction can be represented with the help of the MIF.

The same approach, when applied to synthetically accessible linezolid-like derivatives, indicated that the introduction of a 3-methyl-1,2,4-oxadiazol-5-yl moiety as a C-ring could be a promising modification of the oxazolidinone antibiotics' scaffold. In the present paper we report the synthesis and the *in vitro* antibacterial activity of novel linezolid-like oxadiazoles **1**–**7a**,**b** (Chart 1) to investigate the change in biological activity due to: the replacement of the morpholine ring by the 1,2,4-oxadiazole in the C-ring, the presence of a fluorine substituent in the B-ring, and the variety of substituents on the C(5) side-chain of the oxazolidinone [17].

Additionally, the recently developed algorithm called Fingerprints for Ligands and Proteins (FLAP), that can be used to describe proteins and ligands based on a common reference framework [19], has been used to compare the position of the synthesized active compounds with that of linezolid into the binding site.

Compound	R^1	R^2
1a	H	I
1b	F	I
2a	H	N_3
2b	F	N_3
3a	H	$NHC(=O)CH_3$
3b	F	$NHC(=O)CH_3$
4a	H	$NHC(=S)CH_3$
4b	F	$NHC(=S)CH_3$
5a	H	pyrazol-1-yl
5b	F	pyrazol-1-yl
6a	H	imidazol-1-yl
6b	F	imidazol-1-yl
7a	H	1,2,4-triazol-1-yl
7b	F	1,2,4-triazol-1-yl

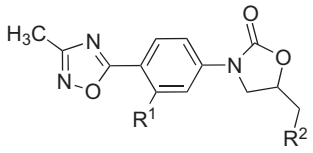

Chart 1.

2. Results and discussion

2.1. Chemistry

In order to prepare the desired scaffold, the synthetic route toward compounds **1**–**7a**,**b** has been planned starting from the oxadiazole end of the molecule by following the classic *amidoxime route* (Scheme 1) [20]. Thus, acetamidoxime **9** was reacted with either mono- or di-fluorobenzoyl chlorides **8a**,**b** producing 5-fluoroarylated 1,2,4-oxadiazoles **10a**,**b**. In the latter compounds, according to previously reported reactivity [21–24], the *para* position of the 5-aryl substituent is activated to undergo a SN_{Ar} with allylamine, yielding compounds **11a**,**b**. Finally, reaction with di-(*t*-butyl)-dicarbonate and subsequent iodocyclocarbamation [25] of the resulting derivatives **12a**,**b**, yielded oxazolidinones**1a**,**b** as ideal precursors for further side-chain modifications.

For the subsequent functionalization, the considered side-chains included the acetamidomethyl moiety (see **3a**,**b**), typical of linezolid, as well as the corresponding thioamide derivatives (**4a**,**b**). Their azide precursors **2a**,**b** were obtained by reaction of compounds **1a**,**b** with sodium azide in dimethylformamide. Subsequent reduction with triphenylphosphine [26] yielded the corresponding amino derivatives **13a**,**b**. After isolation and characterization, the amino derivatives **13** were readily reacted with acetyl chloride, thus avoiding their decomposition, presumably due to oxidative processes occurring upon air exposure. The resulting acetamidomethyl derivatives **3a**,**b**, were finally reacted with the Lawesson's Reagent yielding thioamide derivatives **4a**,**b** (Scheme 2).

Additionally, since the introduction of five-membered heteroaromatic moieties into the C(5) side-chain was shown to maintain or enhance the antibacterial activity [27], the synthesis of compounds **5**–**7a**,**b**, containing various azole rings in the side-chain, was planned.

All compounds **5**–**7a**,**b** were obtained by reaction under solvent-free conditions of the corresponding iodomethylene derivatives **1a**,**b** with pyrazole, imidazole, or 1,2,4-triazole, respectively (Scheme 3). Reaction conditions were carefully chosen in order to avoid the formation of by-products due to β-elimination, as observed in alkaline solution conditions.

2.2. Minimum inhibitory concentration testing

The fourteen new compounds were tested to evaluate their antibacterial activity against both standard references and clinical strains of methicillin-susceptible (MSSA) and methicillin-resistant

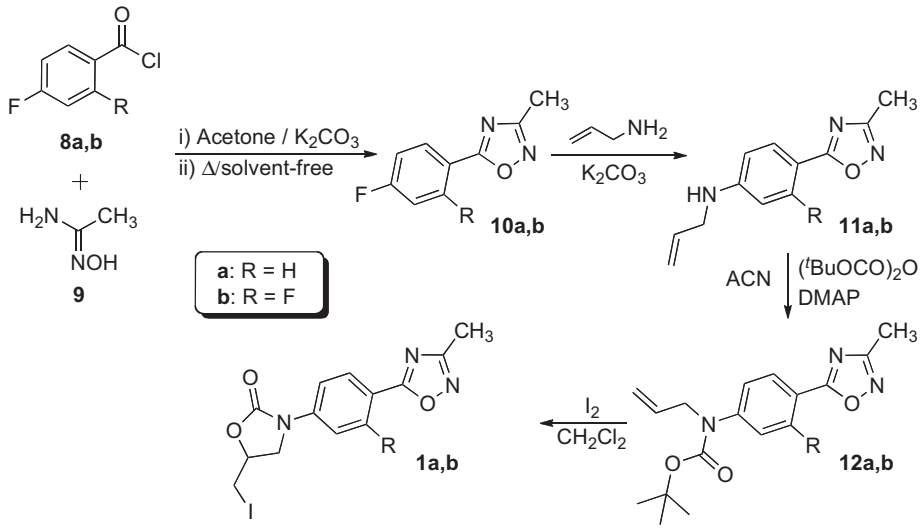

Scheme 1.

S. aureus (MRSA). Antimicrobial activities, summarized in Table 1, were determined by the "gold standard" broth microdilution method using the Clinical and Laboratory Standards Institute (CLSI) recommendations (See Experimental). Minimal Inhibitory Concentrations (MIC) values were expressed in μg/mL and cell viability tests were performed to evaluate the selective antibacterial toxicity of the most active compounds.

Four out of the fourteen tested compounds (see Table 1) showed MIC values against both MSSA and MRSA strains with potency comparable or superior to that of linezolid. Moreover, better activity against MSSA and MRSA as compared to linezolid was shown by the sulfur containing derivatives **4a** and **4b**, whereas compounds **3a**,**b** were less active than linezolid, except for MRSA 433 strain. Comparison with linezolid must take into account that the tested compounds were used as racemic mixture, therefore the antibacterial activity for **3a**, **3b**, **4a** and **4b** is possibly underestimated as compared to the potency of the pure active enantiomer.

2.3. Cell viability assay

To assess if the effect shown against bacterial cells could be related to a selected toxicity or to a more general toxic effect, we performed a first level assay in different types of eukaryotic cell lines to screen the new compounds for their general cytotoxic activity. Data obtained from the first level assay reported below will allow us to select the most promising compounds that in a next-step analysis will be evaluate for the known oxazolidinone mechanisms of toxicity, such as the inhibition of mitochondrial protein synthesis. All tested cell lines were treated with increasing concentrations (5–400 μg/mL) of **4a**, **4b**, and linezolid as reference compound. Another control was DMSO used as solvent. In PK15 (porcine kidney epithelial) cell line, all the tested concentrations of compound **4a** induced a significant reduction ($P < 0.01$) of cells viability. These effects were concentration-dependent (Fig. 2) and the reduction of cell viability reached about 70% at the 100 μg/mL concentration of **4a** and more than 90% cell death at 200 and 400 μg/mL.

Compound **4a** negatively affected also the viability of HaCaT (human keratinocytes) cell line. In fact, it significantly reduced cell viability already at 5 μg/mL ($P < 0.05$) and it induced more than 60% cell death at all concentrations higher or equal to 25 μg/mL ($P < 0.01$) (Fig. 3).

Similar results were obtained using the HepG2 (human hepatocellular carcinoma) cell line (Fig. 4).

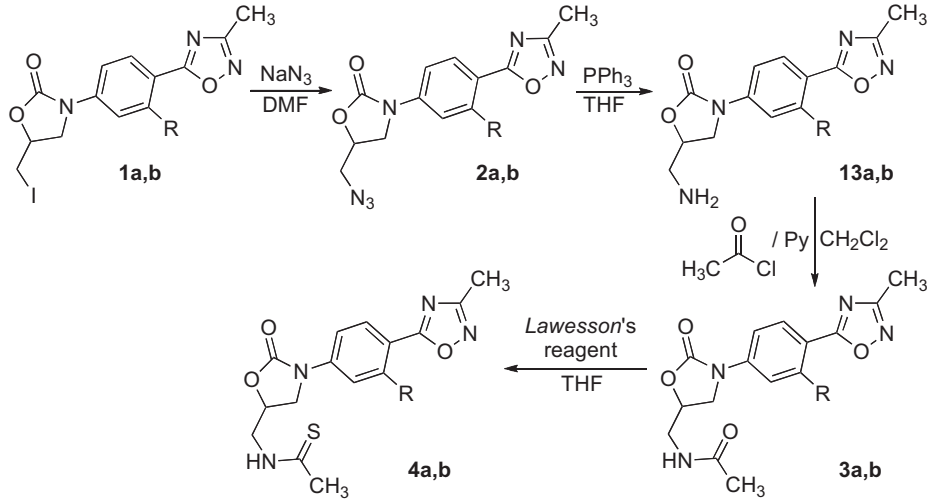

Scheme 2.

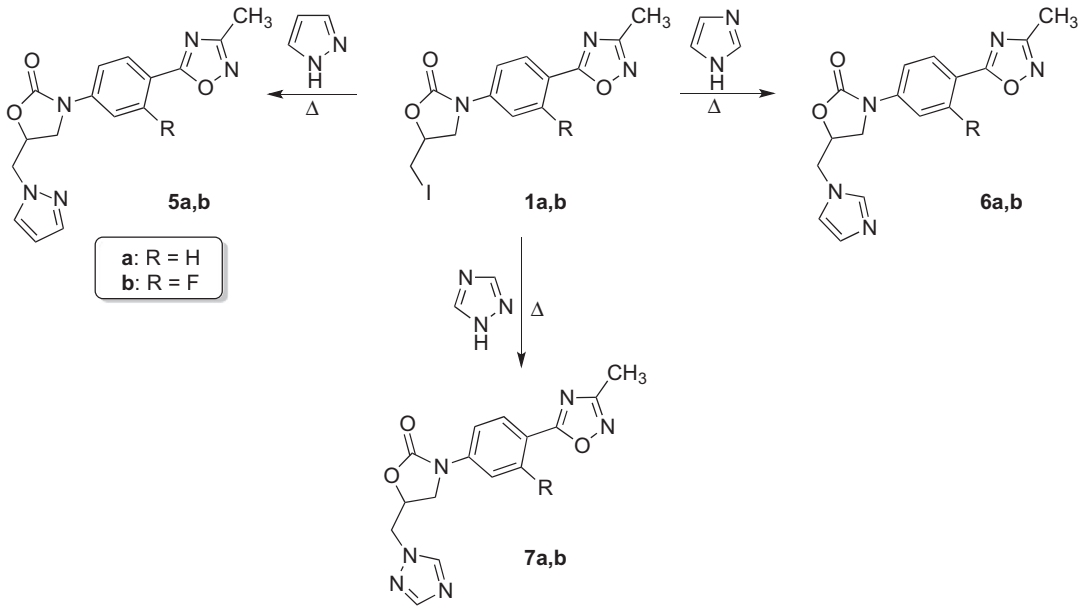

Scheme 3.

Compound **4b** showed a moderate viability reduction (less than 10%) on PK15 cells, which reached statistically significance at the 25 ($P < 0.01$), 50 ($P < 0.05$) and 200 μg/mL ($P < 0.05$) concentrations, respectively (Fig. 2). This trend was comparable to that exhibited by linezolid at the same concentrations.

The reduction of cell viability caused by **4b** was more pronounced in the HaCaT, reaching more than 50% cell death for the 200 and 400 μg/mL concentrations ($P < 0.01$; Fig. 3).

HepG2 cells showed a significant reduction ($P < 0.01$) of viability beginning from the 50 μg/mL of **4b**, with a maximum of toxicity at the 400 μg/mL concentration, with a cellular decrease of about 40% (Fig. 4).

Linezolid demonstrated no viability reduction on PK15 cells, and its 400 μg/mL concentration paradoxically stimulated cell replication ($P < 0.01$; Fig. 2). The cell viability of HaCaT was decreased by incubation with linezolid, with the higher effects at the 200 and 400 μg/mL concentrations ($P < 0.01$; Fig. 3). Interestingly, HepG2 well tolerated the incubation with linezolid, and no negative effects on cell viability were measured (Fig. 4).

Table 1
Antimicrobial activities, expressed in MIC values (μg/mL) of compounds **1**–**7** against MSSA and MRSA strains; linezolid was used as reference antibiotic agent.

Compd	MIC (μg/mL)				
	ATCC 29213	MSSA M923	MRSA MU50	MRSA 433	MRSA F511
1a	>50	>50	50	25	50
1b	>50	>50	50	50	>50
2a	>50	>50	>50	>50	>50
2b	>50	>50	>50	>50	>50
3a	12.5	6.25	6.25	1.6	12.5
3b	12.5	6.25	6.25	1.6	12.5
4a	3.13	1.6	≤0.4	1.6	1.6
4b	1.6	1.6	≤0.4	0.8	1.6
5a	>50	>50	>50	>50	>50
5b	>50	>50	>50	>50	>50
6a	>50	>50	>50	>50	>50
6b	>50	>50	>50	>50	>50
7a	>50	>50	>50	>50	>50
7b	>50	>50	>50	>50	>50
Linezolid	≤0.4	3.13	0.8	1.6	3.13

2.4. Structure–activity relationships

Structure–activity relationship (SAR) for oxazolidinones has been extensively reported. In the case of the 5-acetoamidomethyl moiety, it was previously believed that this group could play a key role on the antimicrobial activity; however, good alternatives such as 1,2,3-triazol-2yl-methyl [28], the pyrid-2-yl-oxymethyl and the isoxazol-3-yl-oxymethyl groups [29] were able to maintain or enhance the antibacterial activity [27]. In this study the substitution of the 5-acetamidomethyl group with other five-membered heterocyclic rings such as 1,2,4-triazole and 1,3-diazole led to a complete loss of the activity against both MSSA and MRSA (see Table 1). A loss of antibacterial activity was also observed for the synthetic precursors where R = I or N_3. On the contrary, the most active compounds reported in the present study (see Chart 2) retain the 5-acetamidomethyl (**3a** and **3b**) or possess the 5-thioacetamidomethyl (**4a** and **4b**) groups.

In particular, the replacement of the acetoamidomethyl group with a thioacetoamidomethyl group led to a 8-fold decrease of the MIC value. This finding confirms results reported by L.M. Thomasco et al. [30] who demonstrated that the 2-aminomethyl thiadiazole oxazolidinones with a thioamide side-chain are extraordinarily potent. In particular, they showed that the 2-aminomethyl-1,3,4-thiadiazolyl phenyl oxazolidinone thioamide (PNU-182347) has MIC values of <0.5 μg/mL against *S. aureus* UC 9213, *S. pneumoniae* UC 9912 and *Haemophilus influenzae* UC 30063. More recently, a series of thiocarbonyl groups such as thioamide, dithiocarbamate, thiourea, and thiocarbamate were tested as possible modifications of the C(5) side-chain of linezolid [31] and those compounds resulted to be *in vivo* more active than linezolid tested as the internal reference.

In addition to the acetoamide group, the 3-(3′-fluorophenyl)-oxazolidinone ring was also considered to play a key role for antimicrobial activity. In particular, in all SAR studies the tendency is to maintain the fluorine atom at the 3 position of the phenyl ring, because for linezolid a fluorine atom at the 3′ position was reported to practically double both *in vitro* and *in vivo* activity [12,32]. *In vivo* studies for linezolid also showed that the addition of a fluorine substituent on the phenyl 3-position in the B-ring eliminated the toxic bone marrow effects, decreased adverse reactions, and enhanced activity [32]. Finally, the size of the 3-substituents is very

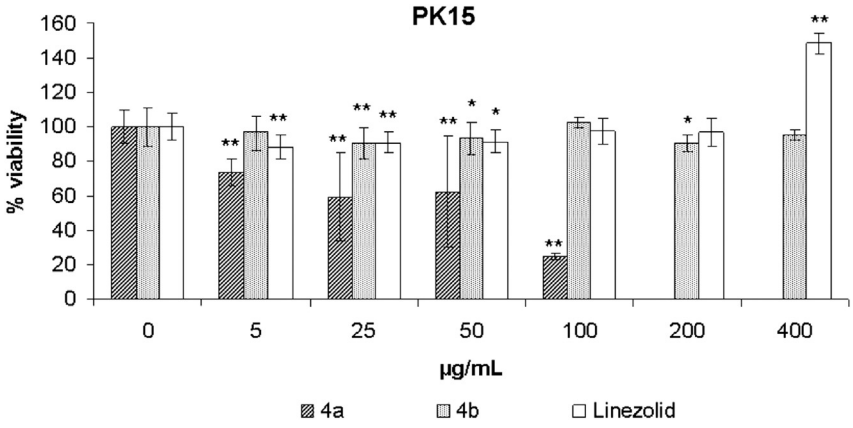

Fig. 2. Cell viability of **4a**, **4b**, and linezolid in PK15 cells. $^{*}P < 0.05$; $^{**}P < 0.01$.

important; the larger the substituent, the lower the antimicrobial activity [33,34].

In this study, a comparison of the antimicrobial activity for **3a** and **3b**, and for **4a** and **4b**, respectively, shows that the fluorine atom in 3 position of the phenyl ring does not play any role when the morpholinic ring of linezolid is replaced with the 1,2,4-oxadiazole ring. Thus, the modification of the C-ring seems to drastically change the SAR behavior of **3a**, **3b**, **4a**, and **4b** with respect to linezolid, although the antimicrobial activity is retained.

3. Modeling studies

An *in silico* study of the binding mode for the tested compounds based on the eubacterial *Deinococcus radiodurans* 50S ribosomal subunit resolved at 3.5 Å in complex with linezolid (pdb code: 3DLL) was performed. Considering the low resolution of the crystal, two independent and complementary approaches were used: a ligand-based method, driven by the X-ray linezolid conformation, and a structure-based approach, only driven by the 50S subunit structure.

3.1. Ligand-based binding mode

To discuss the mechanism of action of the most active compounds, docking studies have been carried out on **3a**, **3b**, **4a**, and **4b** (Chart 2), also comparing their binding position with that of the reference drug, linezolid.

Linezolid binds to Peptidyl Transferase Center (PTC), specifically to the A-site domain, partially overlapping the aminoacyl moiety as many other antibiotics [3]. A model of 23S subunit for *S. aureus* (see Methods) has been made based over the 23S subunit of the *D. radiodurans* 50S ribosomal subunit, in complex with linezolid [3]. Sequence alignment of *D. radiodurans* and *S. aureus* shows that the bases directly involved in the binding site of linezolid are 100% conserved between the two bacteria, allowing the hypothesis that the designed oxadiazole compounds dock at the same spot of linezolid.

Both *R* and *S* stereoisomers of **3a**, **3b**, **4a** and **4b** dock superposing the best conformation of each compound over linezolid, as shown in Fig. 5A–D.

Fig. 5A shows the *S*-enantiomer of **4b**, the most active compound, in complex with *S. aureus*, superposed over linezolid (LZD) in complex with *D. radiodurans*. After minimization, **4b** perfectly overlaps linezolid and small adjustment over *S. aureus* binding site are observed. Designed drugs have an aromatic C-ring moiety, and this difference versus linezolid C-ring confers a more rigid system with delocalized aromaticity between C-ring and B-ring. This results, see Fig. 5B, in a more organized packing of the bases around C and B-rings, A2451, C2452 and U2504 (*Escherichia coli* numbering), that force a small rotation over drug vertical axis with respect to linezolid. B-ring of the tested compounds is tightly sandwiched between A2451 and C2452 and this forces the co-planar C-ring moiety to interact, through hydrogen bonding involving the N(2) of the 1,2,4 oxadiazole moiety with U2585, whose importance in linezolid binding has been documented [3]. The stacking of the oxazolidinone ring moiety (A-ring) with U2504 observed in the crystal structure is also observed in our set of compounds.

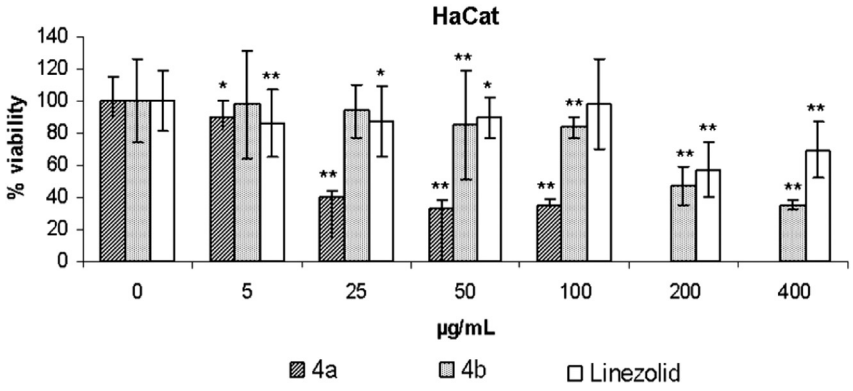

Fig. 3. Cell viability of **4a**, **4b**, and linezolid in HaCaT cells. $^{*}P < 0.05$; $^{**}P < 0.01$.

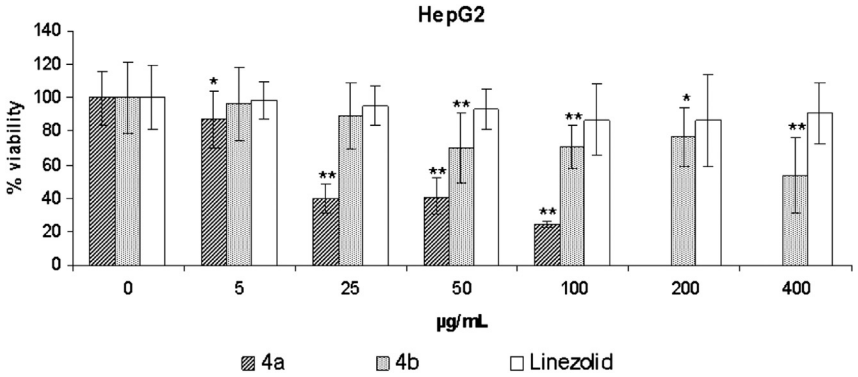

Fig. 4. Cell viability of **4a**, **4b**, and linezolid in HepG2 cells. $^{*}P < 0.05$; $^{**}P < 0.01$.

Designed compounds, thus, share a mostly common binding mode with linezolid. The active role of Mg^{2+} ion is still uncertain, since Wilson et al. discussed about a *putative* Mg ion [3]. However, no clear interaction with magnesium ions could apparently be forecasted in the present case. Nevertheless, by using this ligand-based approach, a possible interaction between **4b**-*S* and Mg^{2+}, due to a coordination involving the thionyl moiety and the F atom, is observed (Fig. 5B).

Resistance to linezolid in *S. aureus* has been associated to mutations in both 23S rRNA and L3 ribosomal protein. In 23S rRNA documented mutations are G2447T, T2500A, T2504A and G2576T [5,35–41], which, unlike U2504, are not in direct contact with the oxazolidinone compounds, but interact with bases involved in drug binding. In fact, T2500 interacts with U2504, which is stacked with the A-ring moiety; G2447 interacts with both C2452 and A2451 which, in our model of *S. aureus*, tightly pack the B-ring moiety; G2576 forms stacking interaction with G2505, that interacts with the C(5) side-chain of the oxazolidinone. In L3 ribosomal protein A157R mutation has been reported [38]. A157 of L3, as seen for most of the 23S rRNA mutants, does not directly interact with linezolid but, again, interacts with both G2505 and U2506, both involved in the binding site. Reported mutations, with the exception of U2504, seem to act as modulators for shape of the binding site, indirectly allowing or hindering linezolid binding. Fig. 5C shows all designed *S*-enantiomers of the tested compounds docked in PTC A-site binding pocket. As shown, no important differences are observed among these drugs, and no relevant changes in binding are observed between the drugs here reported and linezolid. This is due to the absence, to date, of a characterization of the clinical MSSA and MRSA strains used to test our drugs, thus the models do not yet take in consideration the mutated bases of our strains, which actually *make* the difference. The docking study also suggests a higher affinity of *S* stereoisomers for the binding site, which might lead to higher activity of the *S* compounds in the racemic mixture. Indeed, the C(5) side-chain of *R* enantiomers are predicted to clash with U2504 thus forcing a rotation of U2504 base and altering the fundamental stacking interaction of this base with the A-ring. A similar effect has been reported for 23S rRNA crystal structure of *Haloarcula marismortui* in complex with anisomycin [39], which shows a rotated U2504 base, although anisomycin does not occupy the same binding site, and U2504 does not form stacking interactions with any ring of this drug.

3.2. Structure-based binding mode

FLAP structure-based approach was used to investigate the possible binding modes of the four active compounds **3a**, **3b**, **4a**, and **4b**, reported in Chart 2.

FLAP (Fingerprints for Ligands and Proteins) [19,42,43] is a Virtual-Screening and Model-Development method based on 3D molecular similarity, measured through common Molecular Interaction Field (MIF) volumes [44–46]. FLAP is an extremely flexible method that enables a wide variety of applications, from ligand-based Virtual-Screening [47,48] and 3D pharmacophore hypothesis generation [49], to structure based virtual screening [50] and high-throughput proteins pockets clusterization [51].

In this study, the 50S ribosomal subunit from *D. radiodurans* co-crystallized with linezolid (PDB code: 3DLL) [3] was used as a

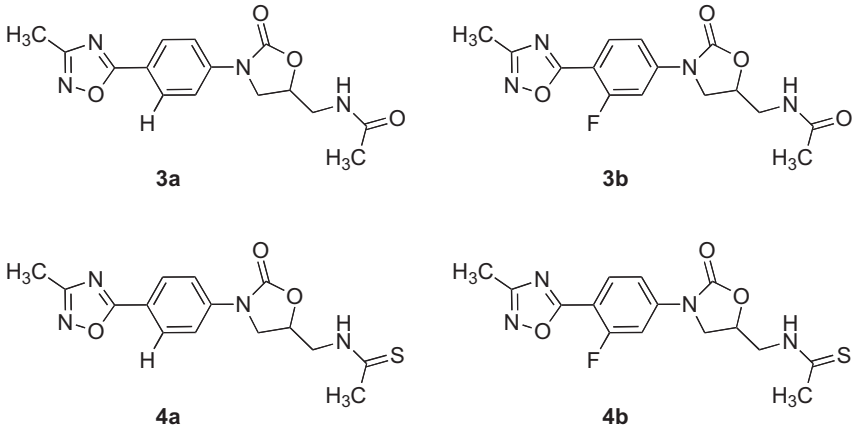

Chart 2.

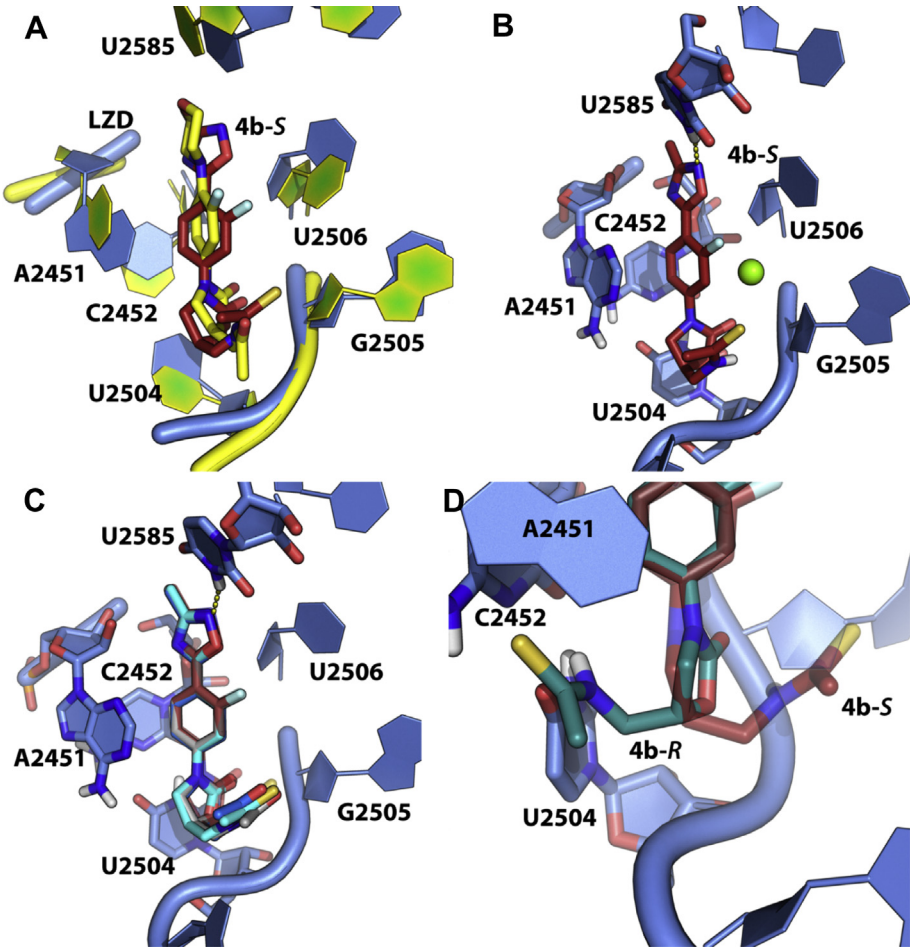

Fig. 5. A) Superimposition of crystal structure of *D. radiodurans* (yellow) 23S subunit binding site in complex with linezolid (ZLD, in yellow sticks) and *S. aureus* model (light blue) in complex with **4b**-*S* (red, in sticks). A small rotation over **4b**-*S* axis is observed with respect to ZLD. B) *S. aureus* in complex with **4b**-*S*, the small rotation observed over ZLD favors a "sandwich-like" stacking of B-ring with A2451 and C2452. As a result, N-(2) of the 1,2,4-oxadiazole directly hydrogen bonds U2585, a key interaction for linezolid activity. C) Superimposition of *S*-stereoisomers of **3a**, **3b**, **4a** and **4b**, all sharing a similar binding mode. D) Difference among *S* (red, in transparency) and *R* (gray) stereoisomers of **4b**. *R* compound might clash with the key base U2504, involved in stacking with the oxazolidinone moiety of linezolid-like compounds. (For interpretation of the references to color in this figure legend, the reader is referred to the web version of this article.)

target. A few X-ray structures of the linezolid-binding site in the 50S subunit have been published so far, and Wilson et al. [3] recently demonstrated that no significant conformational change in the RNA forming binding pocket can be observed upon binding of linezolid, with an exception for U2585. Thus, our target was used as a rigid conformation, having the U2585 in the interactive orientation.

A scheme of the computational procedure is reported in Fig. 6A–C. The X-ray structure of linezolid was removed from the 3DLL structure, and the GRID [46] molecular interaction fields were computed in the cavity.

As expected, the ribosomal cavity is highly polar (blue and red fields), due to several RNA bases able to donate and/or accept Hydrogen-bonds. In the FLAP docking approach, the possible

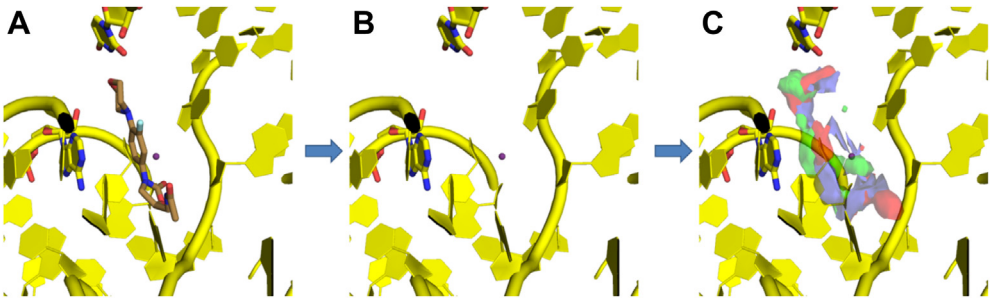

Fig. 6. FLAP structure-based approach. From the crystallographic structure (A), the structure of the co-crystallized linezolid is removed (B). Afterward, the GRID molecular interaction fields were computed in the cavity (C). (Green fields: hydrophobic interaction; blue fields: H-bond donor interaction; red fields: H-bond acceptor interaction). (For interpretation of the references to color in this figure legend, the reader is referred to the web version of this article.)

binding modes of the compounds in the cavity are automatically identified without using the coordinates of the co-crystallized ligand. In fact, starting from a 2D structure of linezolid, FLAP was able to generate a pose possessing high similarity with the cavity interaction fields, and being well superposed to the X-ray structure of linezolid (see Fig. 7).

The same procedure used for linezolid was then repeated for each compound **3a**, **3b**, **4a**, and **4b** with the intent to find their docked conformation and 3D-protein interactions.

Since the measured antimicrobial activity (Table 1) was referred to a racemic mixture, both enantiomers of each structure were included in the dataset. In the structure-based approach, the FLAP software generates the GRID molecular interaction fields (MIFs) both for the ribosomal cavity and for each compound in the dataset, and then it evaluates the similarity between the MIFs of the 50S subunit and those of the compounds. Thus, FLAP automatically selects the conformation and the enantiomeric form for each compound that best fits the cavity. Details for the FLAP procedure are reported in the Experimental section.

In this study, for all the compounds FLAP automatically selected the *S*-enantiomer as the most likely one interacting with the target, according to the ligand-based approach.

Fig. 8A and B shows the best pose for the most active compound **4b** against all the MSSA and MSRA strains.

The pose of compound **4b** suggested by FLAP is very similar to that of the crystallographic linezolid (Fig. 8A). The morpholinic ring is replaced by the N(2) of the 1,2,4-oxadiazole in its H-bond interaction with the nitrogen of U2585, in agreement with the ligand-based results and the crystallographic evidences [3]. Moreover, the methyl group in the 1,2,4-oxadiazole is perfectly oriented toward a hydrophobic region (green color). In this pose the A-ring is differently oriented, and the putative interaction between the Fluorine substituent and the Mg^{2+} ion proposed by Wilson [3] seems not to play a role in this binding mode. The electrostatic interaction of the sulfur atom with the magnesium ion is weak and estimated at about −0.5 kcal using GRID [46]. Looking at the GRID fields (Fig. 8B), due to the different orientation of the A-ring, the stacking with the A2451 is less effective (green region facing this residue). The overall hydrophobic interaction computed by GRID is really weak, and the greatest effect is estimated at only −1.30 kcal/mol, involving the A ring. About the side-chain, the thionyl group is oriented toward a hydroxyl group of the ribose in A2503, and the sulfur–hydroxy hydrogen bond interaction energy computed by GRID is close to −2.0 kcal/mol. The A2503 is not generally ascribed among the critical residues for linezolid binding. Nevertheless, the modification made in the C-ring could favor a possible interaction with A2503. Compounds **3a**, **4a**, and **3b** displayed an analog orientation into the binding site, having the methyl-1,2,4-oxadiazole pointing toward U2585, indicating that neither the lack of the fluorine atom nor the use of an amide groups modify orientation in the cavity (data not shown).

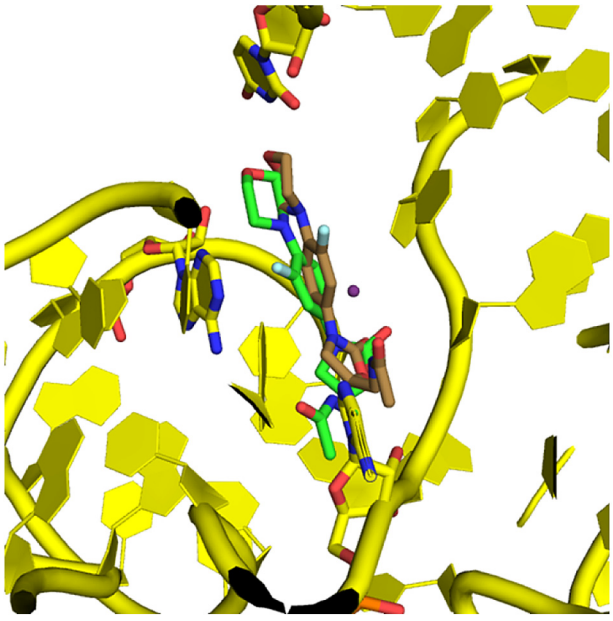

Fig. 7. Comparison of the crystallographic linezolid (in brown) and the FLAP pose (in green). (For interpretation of the references to color in this figure legend, the reader is referred to the web version of this article.)

In order to verify whether the activity of the tested compounds was related to the linezolid-like binding mode, the procedure was repeated for the inactive compound **5b**, in which the side-chain of linezolid was replaced by an pyrazol-1-yl moiety (Fig. 8C and D). The orientation of **5b** is similar to the linezolid X-ray pose and to the computed poses for the tested active compounds, having the 1,2,4 oxadiazole interacting with U2585. This is not surprising considering that all the synthesized compounds mimic the linezolid shape. Nevertheless, the putative interaction with A2503 proposed for the four active compounds is not yet possible not only for **5b** (Fig. 8C and D), but also for all the other inactive compounds in our series. The possible relevance of A2503 in the binding of our linezolid-like 1,2,4-oxadiazole compounds is currently under investigation.

4. Conclusions

Replacement of the linezolid morpholine C-ring with 1,2,4-oxadiazole and the substitution of the carbonyl group with a thionyl one in the side-chain results in the maintenance of the antibacterial activity against *S. aureus* resistant clinical isolates, with a better activity demonstrated against MRSA strains for compound **4b** and a similar cell viability as compared to linezolid. A comparison of the possible binding modes for the tested compounds obtained by two complementary (ligand-based and structure-based) approaches suggests that the binding mode of the tested compounds is very similar to that reported for the ribosome–linezolid complex crystal structure. In particular, the 1,2,4-oxadiazole moiety seems to perfectly mimic the function of the morpholinic ring, since the H-bond interaction with U2585 is retained. This interaction was observed *in silico* for all the tested compounds, despite their activity. However, the performed activity experiments have suggested that the modifications made at the side-chain level could be responsible for the activity. An *in silico* study of the possible interactions of the side chain in the target cavity identified a possible weak interaction with A2503 for the active compounds **3a**, **3b**, **4a**, and **4b**. For all the tested inactive compounds such interaction cannot occur. Thus the possible role of A2503 is currently under investigation.

Fluorination of the phenyl B-ring, reported to improve the antibacterial activity of oxazolidinones with morpholine or piperazine C-ring [11], exhibits a slighter effect in the presence of 1,2,4-oxadiazole as C-ring. Indeed, an effect can be noticed comparing only **4a** and **4b**, thus with a thioacetoamidomethyl moiety as the C(5) side-chain, and only for some strains. Moreover, acetamidomethyl or thioacetoamidomethyl moieties in the C(5) side-chain are essential for activity, likely due to their interactions with the H-bond acceptor region of the ribosomal pocket. On the basis of these experimental evidences and of the modeling information, we hypothesize that the interaction between the F atom and the Mg^{2+} ions for the tested compounds is less important for activity, while a possible interaction of the thionyl group is proposed. However, cell viability studies performed with **4a** and **4b** on three different cell lines of excretory

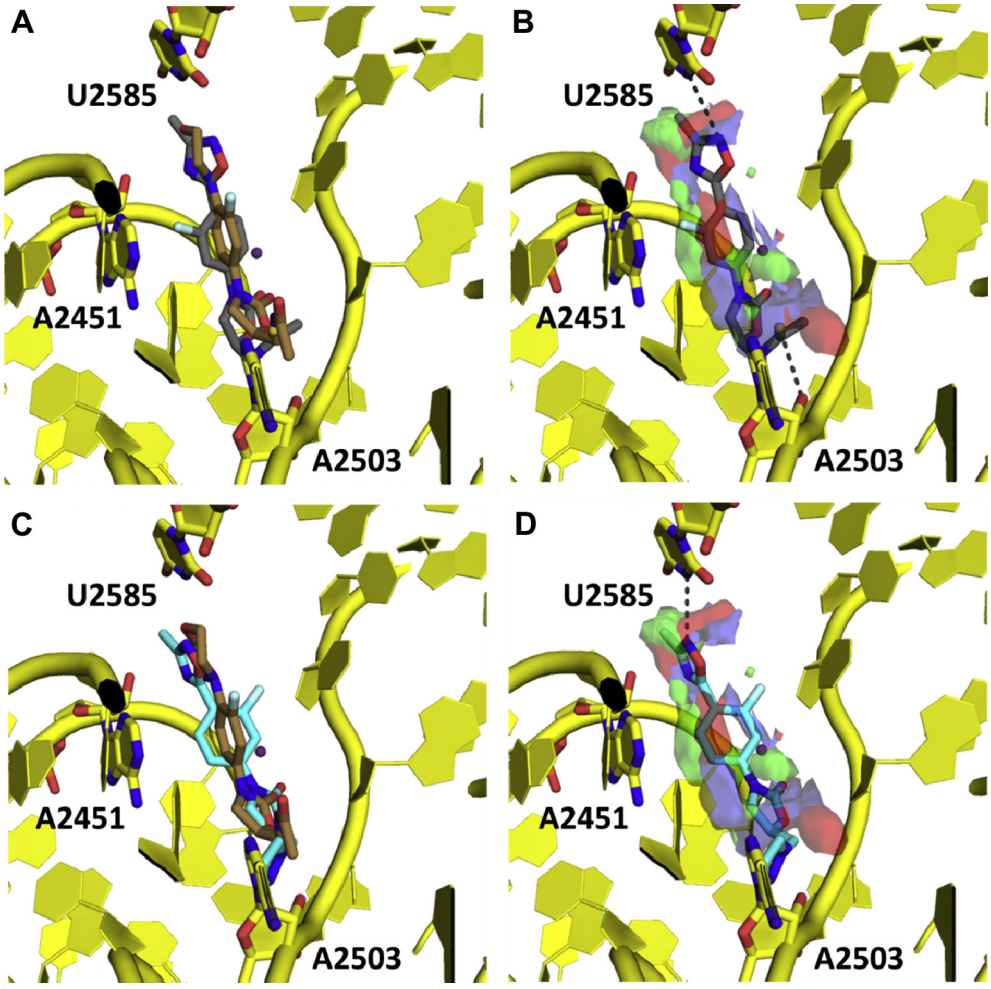

Fig. 8. FLAP poses for **4b** and **5b**. A) Comparison of the X-ray pose for linezolid (brown) and the FLAP pose for **4b** (gray); B) FLAP pose for **4b** according to the GRID fields (green field: hydrophobic interaction; blue fields: H-bond donor interaction; red fields: H-bond acceptor interaction); C) comparison of the X-ray pose for linezolid (brown) and the FLAP pose for 4b (light blue); D) FLAP pose for **5b** according to the GRID fields. (For interpretation of the references to color in this figure legend, the reader is referred to the web version of this article.)

organs demonstrated that the presence of fluorine atom in the phenyl B ring (in **4b**), compared to **4a** in which it is absent, decreases the cytotoxicity to levels similar to those of linezolid. Other modifications seem not to influence the cytotoxicity. Finally, compounds **4a** and **4b** displayed a greater activity with respect to the analogs **3a** and **3b**. It is well-known that thioamide substitutions can improve stability in proteolitic degradation and can also improve ADME properties with respect to the corresponding amide compounds [52]. Thus, whereas thioamides have been considered as an isosteric replacement of amides, the structural differences (i.e., the larger sulfur atom, the elongated C═S bond), the different propensity for hydrogen bond formation and the fact that thioamides are more difficult to hydrolyze than the corresponding amides appear to increase the stability of thioamides in biological systems. The inactive compounds displayed *in silico* a similar binding mode; however, only the interaction with U2585 seems to occur.

5. Experimental section

5.1. Synthesis

5.1.1. Materials and methods

Melting points were determined on a Reichert-Thermovar hot-stage apparatus and are uncorrected. IR spectra (Nujol) were determined with a Shimadzu FTIR-8300 instrument; ^{1}H NMR spectra were recorded on a Bruker 300 Avance spectrometer using TMS as an internal standard. GC–MS determinations were carried out on a Shimadzu GCMS-QP2010 system. Flash chromatography was performed by using silica gel (0.040–0.063 mm) and mixtures of ethyl acetate and petroleum ether (fraction boiling in the range of 40–60 °C) in various ratios. The purity of compounds, in all cases higher than 95%, has been checked by both NMR and HPLC analyses. Elemental analysis (C, H, N) was performed through a vario EL III Element Analyzer, by Elementar Analysensysteme gmbh Hanau, Germany.

5.1.2. General procedure for the preparation of compounds ***10a,b***

A solution of hydroxylamine hydrochloride (1.00 g, 14.4 mmol) and NaOH (0.57 g, 14.4 mmol) in water (5 mL) was added (in about 15 min) to 15 mL of CH_3CN. The reaction mixture was stirred at room temperature for 24 h. The solvent was removed under reduced pressure and the residue treated with ethanol; the resulting suspension was filtered and the solvent was removed under reduced pressure producing 1.659 g of acetamidoxime **9** (77%). Then, either 4-fluorobenzoyl (**8a**) chloride or 2,4-difluorobenzoyl chloride (**8b**) (14.8 mmol) were added to a solution of **9** (1.00 g; 13.5 mmol) in Acetone (35 mL) containing also K_2CO_3 (2.05 g, 14.8 mmol). The mixture was stirred at room temperature for about 90 min after

which the solvent was removed under reduced pressure. The residue was treated with water and the solid precipitate was collected by filtration. The obtained *O*-acylamidoxime was heated, without any further purification, at about 130 °C for 90 min in a sealed tube. The obtained residue was chromatographed yielding the corresponding 1,2,4-oxadiazoles **10a** and **10b**.

*5.1.2.1. 3-Methyl-5-(4′-fluorophenyl)-1,2,4-oxadiazole (**10a**).* Yield (72%); mp 80.0–81.0 °C; ^{1}H NMR (300 MHz; $CDCl_3$) δ 2.45 (s, 3H, Me); 7.16–7.23 (m, 2H, Ar); 8.08–8.14 (m, 2H, Ar). Anal. Found (calc) for $C_9H_7FN_2O$ (%): C, 60.65 (60.67); H, 3.90 (3.96); N, 15.70 (15.72).

*5.1.2.2. 3-Methyl-5-(2′,4′-difluorophenyl)-1,2,4-oxadiazole (**10b**).* Yield (72%); mp 57.0–60.0 °C; ^{1}H NMR (300 MHz; $CDCl_3$) δ 2.46 (s, 3H, Me); 6.95–7.07 (m, 2H, Ar); 8.04–8.14 (m, 1H, Ar). Anal. Found (calc) for $C_9H_6F_2N_2O$ (%): C, 55.15 (55.11); H, 3.10 (3.08); N, 14.25 (14.28).

*5.1.3. Preparation of N-allyl-4-(3′-methyl-1,2,4-oxadiazol-5′-yl)-aniline (**11a**)*

Compound **10a** (0.61 g; 3.43 mmol) was heated, with allylamine (3.0 mL; 2.28 g; 40.0 mmol) and K_2CO_3 (2.00 g; 14.5 mmol), at about 60 °C for 8 days. The reaction mixture was treated with water and extracted with EtOAc. The organic layers were collected, dried over anhydrous Na_2SO_4, filtered and the solvent removed. The residue was chromatographed yielding compound **11a**: Yield (54%); mp 63.9–65.5 °C; IR (Nujol) 3335 (NH), 1607 (C═N) cm^{-1}; ^{1}H NMR (300 MHz; DMSO-d_6) δ 2.31 (s, 3H, Me); 3.76–3.79 (m, 2H, CH_2); 5.12 (dd, 1H, J_1 = 10.5 Hz, J_2 = 1.8 Hz, −CH═CH_2); 5.22 (dd, 1H, J_1 = 17.1 Hz, J_2 = 1.8 Hz, −CH═CH_2); 5.82–5.93 (m, 1H, −CH═CH_2); 6.68 (d, 2H, J = 9.0 Hz, Ar); 6.87 (t, 1H, J = 5.7 Hz, NH, exch. with D_2O); 7.76 (d, 2H, J = 9.0 Hz, Ar). Anal. Found (calc) for $C_{12}H_{13}N_3O$ (%): C, 66.95 (66.96); H, 6.10 (6.09); N, 19.45 (19.52).

*5.1.4. Preparation of N-allyl-3-fluoro-4-(3′-methyl-1,2,4-oxadiazol-5′-yl)-aniline (**11b**)*

To a solution of **10b** (0.86 g; 4.38 mmol) in DMF (2.0 mL) was added allylamine (1.64 mL; 1.25 g; 22.0 mmol). The reaction mixture was stirred for 2 days, after which the solution was treated with water and extracted with EtOAc. The organic layers were collected, dried over anhydrous Na_2SO_4, filtered and the solvent removed. The residue was chromatographed yielding compound **11b**: Yield (49%); mp 57.9–59.9 °C; IR (Nujol) 3335 (NH), 1626 (C═N) cm^{-1}; ^{1}H NMR (300 MHz; DMSO-d_6) δ 2.34 (s, 3H, Me); 3.77–3.81 (m, 2H, CH_2); 5.13 (dd, 1H, J_1 = 13.2 Hz, J_2 = 1.2 Hz, −CH═CH_2); 5.23 (dd, 1H, J_1 = 17.4 Hz, J_2 = 1.2 Hz, −CH═CH_2); 5.81–5.93 (m, 1H, −CH═CH_2); 6.46 (dd, 1H, J_1 = 14.4 Hz, J_2 = 1.8 Hz, Ar); 6.56 (dd, 1H, J_1 = 8.7 Hz, J_2 = 1.8 Hz, Ar); 7.17–7.21 (bs, 1H, NH, exch. with D_2O); 7.72–7.77 (m, 1H, Ar). Anal. Found (calc) for $C_{12}H_{12}FN_3O$ (%): C, 61.80 (61.79); H, 5.10 (5.19); N, 18.15 (18.02).

*5.1.5. General procedure for the preparation of compounds **12a**,**b***

Either compound **11a** or **11b** (2.15 mmol) were dissolved in CH_3CN (25 mL); di-(*t*-butyl)-dicarbonate (0.51 g; 2.36 mmol) and 4-dimethylaminopyridine (0.29 g; 2.36 mmol) were added and the mixture was stirred for 2 days or 2.5 h, respectively. The solvent was removed under reduced pressure and the obtained residue was chromatographed yielding the corresponding compounds **12a** and **12b**.

*5.1.5.1. tert-Butyl-N-allyl-(4-(3′-methyl-1,2,4-oxadiazol-5′-yl)-phenyl)-carbamate (**12a**).* Oil; Yield (73%); IR (Nujol) 1711 (NCO_2), 1614 (C═N) cm^{-1}; ^{1}H NMR (300 MHz; $CDCl_3$) δ 1.27 (s, 9H, *t*-Bu); 2.25 (s, 3H, Me); 4.10 (d, 2H, J = 5.1 Hz, CH_2); 4.95–4.97 (m, 1H, −CH═CH_2); 4.99–5.01 (m, 1H, −CH═CH_2); 5.67–5.78 (m, 1H, −CH═CH_2); 7.23 (d, 2H, J = 9.0 Hz, Ar); 7.84 (d, 2H, J = 9.0 Hz, Ar). Anal. Found (calc) for $C_{17}H_{21}N_3O_3$ (%): C, 64.70 (64.74); H, 6.80 (6.71); N, 13.35 (13.32).

*5.1.5.2. tert-Butyl-N-allyl-(3-fluoro-4-(3′-methyl-1,2,4-oxadiazol-5′-yl)-phenyl)-carbamate (**12b**).* oil; Yield (72%); IR (Nujol) 1713 (NCO_2), 1615 (C═N) cm^{-1}; ^{1}H NMR (300 MHz; $CDCl_3$) δ 1.53 (s, 9H, *t*-Bu); 2.53 (s, 3H, Me); 4.36 (d, 2H, J = 5.1 Hz, CH_2); 5.21–5.28 (m, 2H, −CH═CH_2); 5.91–6.02 (m, 1H, −CH═CH_2); 7.28–7.36 (m, 2H, Ar); 8.02–8.08 (m, 1H, Ar). Anal. Found (calc) for $C_{17}H_{20}FN_3O_3$ (%): C, 61.25 (61.25); H, 6.10 (6.05); N, 12.65 (12.61).

*5.1.6. General procedure for the preparation of compounds **1a**,**b***

To a solution of 1.70 mmol of either compound **12a** or **12b** in CH_2Cl_2 (10 mL) was added I_2 sublimate (1.29 g; 5.10 mmol). The solution was stirred for 24 h, after which the reaction was treated with a solution of Na_2SO_3; the organic layer was dried over anhydrous Na_2SO_4, filtered and the solvent removed. The residue was chromatographed yielding the corresponding compounds **1a** and **1b**.

*5.1.6.1. 3-(4′-(3″-Methyl-1,2,4-oxadiazol-5″-yl)-phenyl)-5-(iodomethyl)-oxazolidin-2-one (**1a**).* Yield (89%); mp 145.0–147.0 °C; IR (Nujol) 1763 (NCO_2), 1618 (C═N) cm^{-1}; ^{1}H NMR (300 MHz; DMSO-d_6) δ 2.47 (s, 3H, Me); 3.62–3.73 (m, 2H, CH_2–I); 3.80 (dd, 1H, J_1 = 9.3 Hz, J_2 = 6.0 Hz, C_4–H); 4.34 (dd, 1H, J_1 = 9.3 Hz, J_2 = 9.0 Hz, C_4–H); 4.81–4.90 (m, 1H, C_5–H); 7.88 (d, 2H, J = 9.0 Hz, Ar); 8.17 (d, 2H, J = 9.0 Hz, Ar). Anal. Found (calc) for $C_{13}H_{12}IN_3O_3$ (%): C, 40.55 (40.54); H, 3.15 (3.14); N, 10.85 (10.91).

*5.1.6.2. 3-(3′-Fluoro-4′-(3″-methyl-1,2,4-oxadiazol-5″-yl)-phenyl)-5-(iodomethyl)-oxazolidin-2-one (**1b**).* Yield (76%); mp 148.0–149.0 °C; IR (Nujol) 1743 (NCO_2), 1637 (C═N) cm^{-1}; ^{1}H NMR (300 MHz; DMSO-d_6) δ 2.48 (s, 3H, Me); 3.61–3.72 (m, 2H, CH_2–I); 3.81 (dd, 1H, J_1 = 9.6 Hz, J_2 = 6.0 Hz, C_4–H); 4.33 (dd, 1H, J_1 = 9.6 Hz, J_2 = 9.0 Hz, C_4–H); 4.83–4.93 (m, 1H, C_5–H); 7.68 (dd, 1H, J_1 = 8.7 Hz, J_2 = 2.1 Hz, Ar); 7.80 (dd, 1H, J_1 = 13.8 Hz, J_2 = 2.1 Hz, Ar); 8.16 (dd, 1H, J_1 = 8.7 Hz, J_2 = 8.5 Hz, Ar). Anal. Found (calc) for $C_{13}H_{11}FIN_3O_3$ (%): C, 38.75 (38.73); H, 2.55 (2.75); N, 10.35 (10.42).

*5.1.7. General procedure for the preparation of compounds **2a**,**b***

To a solution of 0.75 mmol of compound **1a** or **1b** in DMF (6 mL) was added NaN_3 (0.39 g; 6.00 mmol). The solution was stirred for 24 h, after which the reaction was treated with water and extracted with EtOAc; the organic layers were dried over anhydrous Na_2SO_4, filtered and the solvent removed. The residue was chromatographed yielding the corresponding compounds **2a** and **2b**.

*5.1.7.1. 3-(4′-(3″-Methyl-1,2,4-oxadiazol-5-yl)-phenyl)-5-(azidometil)-oxazolidin-2-one (**2a**).* Yield (94%); mp 133.9–135.0 °C; IR (Nujol) 2095 (N_3), 1765 (NCO_2), 1727 (NCO_2), 1618 (C═N) cm^{-1}; ^{1}H NMR (300 MHz; DMSO-d_6) δ 2.46 (s, 3H, Me); 3.75–3.88 (m, 2H, CH_2–N_3); 3.92 (dd, 1H, J_1 = 9.3 Hz, J_2 = 6.0 Hz, C_4–H); 4.28 (t, 1H, J = 9.3 Hz, C_4–H); 4.96–5.03 (m, 1H, C_5–H); 7.86 (d, 2H, J = 9.0 Hz, Ar); 8.16 (d, 2H, J = 9.0 Hz, Ar). Anal. Found (calc) for $C_{13}H_{12}N_6O_3$ (%): C, 52.05 (52.00); H, 4.10 (4.03); N, 27.85 (27.99).

*5.1.7.2. 3-(3′-Fluoro-4′-(3″-methyl-1,2,4-oxadiazol-5-yl)-phenyl)-5-(azidometil)-oxazolidin-2-one (**2b**).* Yield (99%); mp 126.2–127.7 °C; IR (Nujol) 2107 (N_3), 1758 (NCO_2), 1743 (NCO_2), 1630 (C═N) cm^{-1}; ^{1}H NMR (300 MHz; DMSO-d_6) δ 2.41 (s, 3H, Me); 3.69–3.82 (m, 2H, CH_2–N_3); 3.86 (dd, 1H, J_1 = 9.3 Hz, J_2 = 6.0 Hz, C_4–H); 4.21 (t, 1H, J = 9.3 Hz, C_4–H); 4.91–4.99 (m, 1H, C_5–H); 7.60 (dd, 1H, J_1 = 9.0 Hz, J_2 = 1.8 Hz, Ar); 7.72 (dd, 1H, J_1 = 13.5 Hz, J_2 = 1.8 Hz, Ar); 8.08–8.14 (m, 1H, Ar). Anal. Found (calc) for $C_{13}H_{11}FN_6O_3$ (%): C, 49.10 (49.06); H, 3.50 (3.48); N, 26.45 (26.41).

*5.1.8. General procedure for the preparation of compounds **13a**,**b***

To a solution of 0.45 mmol of compound **2a** or **2b** in THF (15 mL) was added PPh_3 (0.16 g; 0.60 mmol). The solution was stirred for about 90 min, after which 100 μl of distilled water was added and the resulting mixture was refluxed for 4 h. The THF was removed under reduced pressure, the resulting residue was neutralized with hydrochloric acid and extracted with EtOAc. A solution of NaOH (pH ~9) was added to the aqueous phase, which was extracted with EtOAc; the organic layers were dried over anhydrous Na_2SO_4, filtered and the solvent removed, yielding the corresponding compounds **13a** and **13b**.

*5.1.8.1. 3-(4′-(3″-Methyl-1,2,4-oxadiazol-5-yl)-phenyl)-5-(aminomethyl)-oxazolidin-2-one (**13a**).* Yield (66%); mp 139.3–141.3 °C; IR (Nujol) 3390 (NH), 3361 (NH), 1748 (NCO_2), 1616 (C=N) cm^{-1}; ^1H NMR (300 MHz; DMSO-d_6) δ 2.22 (bs, 2H, NH_2, exch. with D_2O); 2.39 (s, 3H, Me); 2.77–2.91 (m, 2H, CH_2–NH_2); 3.94 (dd, 1H, $J_1 = 9.0$ Hz, $J_2 = 6.3$ Hz, C_4–H); 4.13 (t, 1H, $J = 9.0$ Hz, C_4–H); 4.61–4.70 (m, 1H, C_5–H); 7.80 (d, 2H, $J = 9.0$ Hz, Ar); 8.09 (d, 2H, $J = 9.0$ Hz, Ar). Anal. Found (calc) for $C_{13}H_{14}N_4O_3$ (%): C, 56.90 (56.93); H, 5.15 (5.14); N, 20.45 (20.43).

*5.1.8.2. 3-(3′-Fluoro-4′-(3″-methyl-1,2,4-oxadiazol-5-yl)-phenyl)-5-(aminomethyl)-oxazolidin-2-one (**13b**).* Yield (88%); mp 137.0–140.0 °C; IR (Nujol) 3372 (NH), 1743 (NCO_2), 1630 (C=N) cm^{-1}; ^1H NMR (300 MHz; DMSO-d_6) δ 2.21 (bs, 2H, NH_2, exch. with D_2O); 2.41 (s, 3H, Me); 2.77–2.91 (m, 2H, CH_2–NH_2); 3.93 (dd, 1H, $J_1 = 9.3$ Hz, $J_2 = 6.3$ Hz, C_4–H); 4.13 (t, 1H, $J = 9.0$ Hz, C_4–H); 4.63–4.71 (m, 1H, C_5–H); 7.60 (dd, 1H, $J_1 = 9.0$ Hz, $J_2 = 2.1$ Hz, Ar); 7.73 (dd, 1H, $J_1 = 10.8$ Hz, $J_2 = 2.1$ Hz, Ar); 8.08–8.14 (m, 1H, Ar). Anal. Found (calc) for $C_{13}H_{13}FN_4O_3$ (%): C, 53.40 (53.42); H, 4.45 (4.48); N, 19.25 (19.17).

*5.1.9. General procedure for the preparation of compounds **3a**,**b***

Acetyl chloride (40 μl; 44 mg; 0.56 mmol) was added to a solution of either compound **13a** or **13b** (0.28 mmol) in CH_2Cl_2 (3 mL) containing also pyridine (1 mL; 0.97 g; 12.3 mmol). The solution was stirred for 30 min after which the solvent was removed and the residue treated with HCl 1 M (20 mL) and extracted with EtOAc; the organic layers were dried over anhydrous Na_2SO_4, filtered and the solvent removed. The residue was chromatographed yielding the corresponding compounds **3a** and **3b**.

*5.1.9.1. 3-(4′-(3″-Methyl-1,2,4-oxadiazol-5-yl)-phenyl)-5-(N-acetylaminomethyl)-oxazolidin-2-one (**3a**).* Yield (58%); mp 214.0–216.0 °C; IR (Nujol) 3257 (NH), 1751 (NCO_2), 1646 (amide), 1616 (C=N) cm^{-1}; ^1H NMR (300 MHz; DMSO-d_6) δ 1.89 (s, 3H, COMe); 2.46 (s, 3H, Me); 3.50 (t, 2H, $J = 5.7$ Hz, CH_2–NHCOMe); 3.88 (dd, 1H, $J_1 = 9.0$ Hz, $J_2 = 6.6$ Hz, C_4–H); 4.25 (t, 1H, $J = 9.0$ Hz, C_4–H); 4.79–4.87 (m, 1H, C_5–H); 7.84 (d, 2H, $J = 8.7$ Hz, Ar); 8.16 (d, 2H, $J = 8.7$ Hz, Ar); 8.32 (t, 1H, $J = 5.7$ Hz, NH, exch. with D_2O); ^{13}C NMR (75 MHz; DMSO-d_6) δ 11.4, 22.6, 41.5, 47.2, 72.0, 118.1 (overlapped signals), 128.9, 142.6, 154.1, 167.7, 170.2, 174.5. Anal. Found (calc) for $C_{15}H_{16}N_4O_4$ (%): C, 56.95 (56.96); H, 5.05 (5.10); N, 17.85 (17.71).

*5.1.9.2. 3-(3′-Fluoro-4′-(3″-methyl-1,2,4-oxadiazol-5-yl)-phenyl)-5-(N-acetylaminomethyl)-oxazolidin-2-one (**3b**).* Yield (62%); mp 184.0–186.0 °C; IR (Nujol) 3343 (NH), 1751 (NCO_2), 1666 (amide), 1628 (C=N) cm^{-1}; ^1H NMR (300 MHz; DMSO-d_6) δ 1.89 (s, 3H, COMe); 2.48 (s, 3H, Me); 3.50 (t, 2H, $J = 5.4$ Hz, CH_2–NHCOMe); 3.88 (dd, 1H, $J_1 = 9.3$ Hz, $J_2 = 6.3$ Hz, C_4–H); 4.25 (t, 1H, $J = 9.0$ Hz, C_4–H); 4.81–4.88 (m, 1H, C_5–H); 7.64 (dd, 1H, $J_1 = 9.0$ Hz, $J_2 = 1.8$ Hz, Ar); 7.77 (dd, 1H, $J_1 = 13.8$ Hz, $J_2 = 1.8$ Hz, Ar); 8.15–8.21 (m, 1H, Ar), 8.31 (m, 1H, NH, exch. with D_2O); ^{13}C NMR (75 MHz; DMSO-d_6) δ 11.32, 22.6, 41.5, 47.3, 72.2, 105.7 (d, $J_{C-F} = 32$ Hz), 106.2 (d, $J_{C-F} = 14$ Hz), 114.1, 131.4, 144.3 (d, $J_{C-F} = 14$ Hz), 153.9, 160.4 (d, $J_{C-F} = 305$ Hz), 167.5, 170.2, 171.6. Anal. Found (calc) for $C_{15}H_{15}FN_4O_4$ (%): C, 53.90 (53.89); H, 4.65 (4.52); N, 16.65 (16.76).

*5.1.10. General procedure for the preparation of compounds **4a**,**b***

The Lawesson's reagent (0.2 g; 0.49 mmol) was added to a solution of either **3a** or **3b** (0.49 mmol) in THF (14 mL). The reaction mixture was refluxed for 2 h, after which the solvent was removed under reduced pressure. The residue was chromatographed yielding the corresponding compounds **4a** and **4b**.

*5.1.10.1. 3-(4′-(3″-Methyl-1,2,4-oxadiazol-5-yl)-phenyl)-5-(N-thioacetylaminomethyl)-oxazolidin-2-one (**4a**).* Yield (77%); mp 199.4–201.0 °C; IR (Nujol) 3217 (NH), 1721 (NCO_2), 1618 (thioamide) cm^{-1}; ^1H NMR (300 MHz; DMSO-d_6) δ 2.47 (s, 3H, Me); 2.51 (s, 3H, CSMe); 3.95–4.03 (m, 3H, overlapped signals); 4.28–4.34 (m, 1H, C_4–H); 5.01–5.11 (m, 1H, C_5–H); 7.85 (d, 2H, $J = 9.0$ Hz, Ar); 8.18 (d, 2H, $J = 9.0$ Hz, Ar); 10.45 (bs, 1H, NH, exch. with D_2O). Anal. Found (calc) for $C_{15}H_{16}N_4O_3S$ (%): C, 54.15 (54.20); H, 4.85 (4.85); N, 16.90 (16.86).

*5.1.10.2. 3-(3′-Fluoro-4′-(3″-methyl-1,2,4-oxadiazol-5-yl)-phenyl)-5-(N-thioacetylaminomethyl)-oxazolidin-2-one (**4b**).* Yield (93%); mp 166.5–167.7 °C; IR (Nujol) 3262 (NH), 1746 (NCO_2), 1633 (thioamide) cm^{-1}; ^1H NMR (300 MHz; DMSO-d_6) δ 2.48 (s, 3H, Me); 2.51 (s, 3H, CSMe); 3.94–4.00 (m, 3H, overlapped signals); 4.28–4.34 (m, 1H, C_4–H); 5.04–5.12 (m, 1H, C_5–H); 7.65 (dd, 1H, $J_1 = 9$ Hz, $J_2 = 1.8$ Hz, Ar); 7.78 (dd, 1H, $J_1 = 13.5$ Hz, $J_2 = 1.8$ Hz, Ar); 8.16–8.22 (m, 1H, Ar); 10.45 (bs, 1H, NH exch. with D_2O). Anal. Found (calc) for $C_{15}H_{14}FN_4O_3S$ (%): C, 51.35 (51.42); H, 4.30 (4.32); N, 16.05 (15.99).

*5.1.11. General procedure for the preparation of compounds **5a**,**b** and **6a**,**b***

Either **1a** or **1b** (0.26 mmol) was heated in presence of pyrazole or imidazole (0.18 g; 2.6 mmol) for 30 min. The mixture was recovered with EtOAc and the solvent removed under reduced pressure. The residue was chromatographed yielding the corresponding compounds **5a**,**b** and **6a**,**b**.

*5.1.11.1. 3-(4′-(3″-Methyl-1,2,4-oxadiazol-5-yl)-phenyl)-5-((pyrazol-1-yl)-methyl)-oxazolidin-2-one (**5a**).* Yield (56%); mp 192.2–194.5 °C; IR (Nujol) 1745 (NCO_2), 1618 (C=N) cm^{-1}; ^1H NMR (300 MHz; $CDCl_3$) δ 2.53 (s, 3H, Me); 4.16–4.30 (m, 2H, C_4–H); 4.60–4.62 (m, 2H, CH_2–pyrazole); 5.08–5.16 (m, 1H, C_5–H); 6.36–6.38 (m, 1H, Pyrazole C_3–H); 7.55 (d, 1H, $J = 1.5$ Hz, Pyrazole C_4–H); 7.64 (d, 1H, $J = 1.5$ Hz, Pyrazole C_5–H); 7.70 (d, 2H, $J = 9.6$ Hz, Ar), 8.15 (d, 2H, $J = 9.6$ Hz, Ar). Anal. Found (calc) for $C_{16}H_{15}N_5O_3$ (%): C, 59.10 (59.07); H, 4.70 (4.65); N, 21.45 (21.53).

*5.1.11.2. 3-(3′-Fluoro-4′-(3″-methyl-1,2,4-oxadiazol-5-yl)-phenyl)-5-((pyrazol-1-yl)-methyl)-oxazolidin-2-one (**5b**).* Yield (40%); mp 179.2–181.0 °C; IR (Nujol) 1745 (NCO_2) cm^{-1}; ^1H NMR (300 MHz; $CDCl_3$) δ 2.55 (s, 3H, Me); 4.19–4.22 (m, 2H, C_4–H); 4.60–4.62 (m, 2H, CH_2–pyrazole); 5.09–5.17 (m, 1H, C_5–H); 6.36–6.37 (m, 1H, Pyrazole C_3–H); 7.35–7.38 (m, 1H, Ar); 7.54 (d, 1H, $J = 1.8$ Hz, Pyrazole C_4–H); 7.59–7.64 (m, 2H, overlapped signals), 8.08–8.14 (m, 1H, Ar). Anal. Found (calc) for $C_{16}H_{14}FN_5O_3$ (%): C, 56.00 (55.98); H, 4.10 (4.11); N, 20.35 (20.40).

*5.1.11.3. 3-(4′-(3″-Methyl-1,2,4-oxadiazol-5-yl)-phenyl)-5-((imidazol-1-yl)-methyl)-oxazolidin-2-one (**6a**).* Yield (72%); mp 206.0–209.0 °C; IR (Nujol) 1747 (NCO_2) cm^{-1}; ^1H NMR (300 MHz; DMSO-d_6) δ 2.46 (s, 3H); 3.95 (dd, 1H, $J_1 = 9.3$ Hz, $J_2 = 6.0$ Hz, C_4–H); 4.28–4.34 (t, 1H, $J = 9.3$ Hz, C_4–H); 4.47–4.49 (m, 2H, CH_2–imidazole); 5.06–5.14 (m, 1H, C_5–H); 6.98 (s, 1H, Imidazole C_5–H); 7.30 (s, 1H,

Imidazole C_4–H); 7.76 (s, 1H, Imidazole C_2–H); 7.81 (d, 2H $J = 8.7$ Hz, Ar); 8.15 (d, 2H, $J = 8.7$ Hz, Ar). Anal. Found (calc) for $C_{16}H_{15}N_5O_3$ (%): C, 59.10 (59.07); H, 4.65 (4.65); N, 21.55 (21.53).

*5.1.11.4. 3-(3′-Fluoro-4′-(3″-methyl-1,2,4-oxadiazol-5-yl)-phenyl)-5-((imidazol-1-yl)-methyl)-oxazolidin-2-one (**6b**).* Yield (55%); mp 185.6–188.9 °C; IR (Nujol) 1748 (NCO_2) cm^{-1}; ^1H NMR (300 MHz; DMSO-d_6) δ 2.48 (s, 3H, Me); 3.96 (dd, 1H, $J_1 = 9.3$ Hz, $J_2 = 6.0$ Hz, C_4–H); 4.28–4.34 (m, 1H, $J = 9.3$ Hz, C_4–H); 4.47–4.48 (m, 2H, CH_2–imidazole); 5.07–5.16 (m, 1H, C_5–H); 6.97 (s, 1H, Imidazole C_5–H); 7.30 (s, 1H, Imidazole C_4–H); 7.62–7.77 (m, 3H, overlapped signals); 8.16–8.22 (m, 1H, Ar). Anal. Found (calc) for $C_{16}H_{14}FN_5O_3$ (%): C, 55.95 (55.98); H, 4.10 (4.11); N, 20.40 (20.40).

*5.1.12. General procedure for the preparation of compounds **7a**,**b***

Either **1a** or **1b** (0.45 mmol) was heated in the presence of 1,2,4-triazole (0.12 g; 1.8 mmol) for 1 h. The mixture was recovered with EtOAc and the solvent removed under reduced pressure. The residue was chromatographed yielding the corresponding compounds **7a** and **7b**.

*5.1.12.1. 3-(4′-(3″-Methyl-1,2,4-oxadiazol-5-yl)-phenyl)-5-((1,2,4-triazol-1-yl)-methyl)-oxazolidin-2-one (**7a**).* Yield (73%); mp 208.0–210.0 °C; IR (Nujol) 1751 (NCO_2) cm^{-1}; ^1H NMR (300 MHz; $CDCl_3$) δ 2.48 (s, 3H, Me); 4.13 (dd, 1H, $J_1 = 9.0$ Hz, $J_2 = 6.1$ Hz, C_4–H); 4.25 (t, 1H, $J = 9.0$ Hz, C_4–H); 4.59–4.61 (m, 2H, CH_2–triazole); 5.06–5.12 (m, 1H, C_5–H); 7.64 (d, 2H, $J = 9.0$ Hz, Ar); 7.96 (s, 1H, Triazole C_3–H); 8.12 (d, 2H, $J = 9.0$ Hz, Ar); 8.26 (s, 1H, Triazole C_5–H). Anal. Found (calc) for $C_{15}H_{14}N_6O_3$ (%): C, 55.20 (55.21); H, 4.30 (4.32); N, 25.70 (25.75).

*5.1.12.2. 3-(3′-Fluoro-4′-(3″-methyl-1,2,4-oxadiazol-5-yl)-phenyl)-5-((1,2,4-triazol-1-yl)-methyl)-oxazolidin-2-one (**7b**).* Yield (64%); mp 176.2–177.8 °C; IR (Nujol) 1751 (NCO_2) cm^{-1}; ^1H NMR (300 MHz; $CDCl_3$) δ 2.48 (s, 3H, Me); 4.07 (dd, 1H, $J_1 = 9.5$ Hz, $J_2 = 5.7$ Hz, C_4–H); 4.31–4.39 (m, 1H, $J = 9.5$ Hz, C_4–H); 4.61–4.79 (m, 2H, CH_2–triazole); 5.15–5.27 (m, 1H, C_5–H); 7.60 (dd, 1H, $J_1 = 9.0$ Hz, $J_2 = 2.2$ Hz, Ar); 7.73 (dd, 1H, $J_1 = 13.5$ Hz, $J_2 = 2.0$ Hz, Ar); 8.07 (s, 1H, Triazole C_3–H); 8.14–8.21 (m, 1H, Ar) 8.64 (s, 1H, Triazole C_5–H). Anal. Found (calc) for $C_{15}H_{13}FN_6O_3$ (%): C, 52.35 (52.33); H, 3.80 (3.81); N, 20.45 (24.41).

5.2. Microbiological assays

5.2.1. Bacterial strains

A total of 5 (2 MSSA and 3 MRSA) well characterized for their antibiotic-susceptibility phenotype *S. aureus* isolates were used for the determination of the *in vitro* antibacterial activity of the studied compounds. In particular, *S. aureus* ATCC 29213 reference standard strain and *S. aureus* M923 (collection strain) were used as MSSA strains. Among MRSA, *S. aureus* MU50 (ATCC 700699) reference standard strain and two collection strains (433 and F511) were used for susceptibility assays.

5.2.2. Determination of minimum inhibitory concentrations (MICs)

The *in vitro* antibacterial activity of the new agents was studied by determining their minimum inhibitory concentrations (MICs) by means of the broth microdilution method according to the Clinical and Laboratory Standards Institute (CLSI) guidelines [53]. Briefly, serial 2-fold dilutions of each compound were made using the Mueller–Hinton broth in microtitre plates with 96 wells. Dimethyl sulfoxide (DMSO) was used as solvent for all the synthetized compounds. An equal volume of the bacterial inoculum (1×10^6 CFU/mL) was added to each well on the microtitre plate containing 0.05 mL of the serial antibiotic dilutions. The microtitre plate was then incubated at 37 °C for 18–24 h after which each well was analyzed for the presence of bacterial growth. The MIC was defined as the lowest concentration of antimicrobial agent able to cause inhibition of bacterial growth as shown by the lack of turbidity of the culture medium. The *in vitro* antibacterial activities of 14 new linezolid-like 1,2,4-oxadiazoles were tested and compared to that of reference oxazolidinone in clinical use: linezolid (Zyvox(R), Pfizer in Sigma-Aldrich, Italy). Final DMSO concentrations were also taken into account in all the biological assays.

5.2.3. Cell viability assay

The effects of **4a**, **4b**, and linezolid on cells viability were studied *in vitro* on PK15 (porcine kidney epithelial), HaCaT (human keratinocytes), and HepG2 (human hepatocellular carcinoma) cell lines [54–56]. HepG2 and HaCat cells were grown in Dulbecco's modified eagles medium (DMEM) whereas PK15 in DMEM/M199 (1:1). All media were supplemented with 10% heat inactivated fetal bovine serum (FBS), 2 mM L-glutamine, 100 units/mL penicillin and 100 μg/mL streptomycin. Cells were maintained at 37 °C in a 5% CO_2 atmosphere. All reagents for cell culture were from Euroclone (Pero, Italy).

Cell viability was measured by the MTT assay [57]. Briefly, MTT [3-(4,5-Dimethythiazol-2-yl)-2,5-diphenyltetrazolium bromide] stock solution (5 mg/mL) was added to each well to a final concentration of 1.2 mM, and cells were incubated for 1 h and 30 min at 37 °C. After removing MTT solution, the reaction was stopped by adding 90% ethanol. Resuspended cells were centrifuged 10 min at 800× *g*. The absorbance was measured with the multilabel Victor^3 spectrophotometer (Perkin Elmer, Turku, Finland) at wavelength of 570 nm. Data are means ± S.E. of 3 separate experiments performed in triplicate.

5.2.4. Statistical analysis

Statistical significance was obtained with Student's *t* test in comparison with controls $^*\underline{P} < 0.05$, $^{**}\underline{P} < 0.001$. Data are means ± S.E. of 3 separate experiments performed in triplicate.

6. Computational methods

6.1. Methods

6.1.1. Ligand-based approach

The model of wild type *S. aureus* 23S ribosomal rRNA (genebank id: X68425) has been made with mode RNA program [58] using as a template the 23S subunits of the 50S rRNA subunit of *D. radiodurans* (pdb ID: 3DLL).

3a, **3b**, **4a** and **4b** molecules, as the most representative compounds of this study, have been drawn, in both *R* and *S* stereoisomers, with MOE [59]. Minimization and a conformational analysis of the compounds have been performed with the same program. The complexes of *S. aureus* 23S ribosomal rRNA with drawn drugs **3a**,**b** and **4a**,**b** have been made taking in consideration the similarity between designed compounds and linezolid, thus docking have been made manually, superposing the best conformations over linezolid, using PyMOL [60]. The general Amber force field [61] and HF/6-31G*-derived RESP atomic charges were used for the ligands. Minimizations of complexes have been performed with the Sander module of AMBER10 [62,63]. Restrictions over atoms farther than 20 Å from binding site have been applied.

6.1.2. Structure-based approach

The computational tools employed in this work are mainly part of FLAP package [19]. A number of applications of FLAP for virtual-screening was already reported, and its use as Model-Development program was recently published [64]. In this paper, FLAP was used

in the structure-based mode and the template is the protein cavity obtained removing the linezolid molecule from the 3DLL X-ray structure. FLAP compares the MIFs of the cavity to those of **4b**. The original probes used in this analysis were the default probes DRY, O, N1 and H.

Acknowledgments

The authors thank Dr. Elena Lonati and Dr. Antonio Torsello for their contribution in cell viability experiments.

Financial supports from the Italian MIUR within the "FIRB-Futuro in Ricerca 2008" Program – Project n. RBFR08A9V1 (to A.P., C.G.F. and R.M.) and from the University of Catania for a post-doctoral Fellowship (to L.G.) are gratefully acknowledged.

References

[1] Infectious Diseases Society of America, The 10 × '20 initiative: pursuing a global commitment to develop 10 new antibacterial drugs by 2020, Clin. Infect. Dis. 50 (2010) 2081–2083.
[2] C. Zou, L. Zhou, Mol. Simul. 33 (2007) 517–530.
[3] D.N. Wilson, F. Schluenzen, J.M. Harms, A.L. Starosta, S.R. Connell, P. Fucini, Proc. Natl. Acad. Sci. U. S. A. 105 (2008) 13339–13344.
[4] J.A. Ippolito, Z.F. Kanyo, D. Wang, F.J. Franceschi, P.B. Moore, T.A. Steitz, E.M. Duffy, J. Med. Chem. 51 (2008) 3353–3356.
[5] S. Tsiodras, H.S. Gold, G. Sakoulas, G.M. Eliopoulos, C. Wennersten, L. Venkataraman, R.C. Moellering, M.J. Ferraro, Lancet 358 (2001) 207–208.
[6] C. Auckland, L. Teare, F. Cooke, M.E. Kaufmann, M. Warner, G. Jones, K. Bamford, H. Ayles, A.P. Johnson, J. Antimicrob. Chemother. 50 (2002) 743–746.
[7] J. Seedat, G. Zick, I. Klare, C. Konstabel, N. Weiler, H. Sahly, Antimicrob. Agents Chemother. 50 (2006) 4217–4219.
[8] S. Kelly, J. Collins, M. Maguire, C. Gowing, M. Flanagan, M. Donnelly, P.G. Murphy, J. Antimicrob. Chemother. 61 (2008) 901–907.
[9] J.V.N. Vara Prasad, Curr. Opin. Microbiol. 10 (2007) 454–460.
[10] D.K. Hutchinson, Curr. Top. Med. Chem. 3 (2003) 1021–1042.
[11] M.B. Gravestock, Curr. Opin. Drug Discov. Dev. 8 (2005) 469–477.
[12] M.R. Barbachyn, C.W. Ford, Angew. Chem. Int. Ed. 42 (2003) 2010–2023.
[13] A.R. Renslo, G.W. Luehr, M.F. Gordeev, Bioorg. Med. Chem. 14 (2006) 4227–4240.
[14] Y.W. Jo, W.B. Im, J.K. Rhee, M.J. Shim, W.B. Kim, E.C. Choi, Bioorg. Med. Chem. 12 (2004) 5909–5915.
[15] C. Farrerons Gallemi, US Patent 2005/0014806, 2005.
[16] L.B. Snyder, Z. Meng, R. Mate, S.V. D'Andrea, A. Marinier, et al., Bioorg. Med. Chem. Lett. 14 (2004) 4735–4739.
[17] A. Palumbo Piccionello, R. Musumeci, C. Cocuzza, C.G. Fortuna, A. Guarcello, P. Pierro, A. Pace, Eur. J. Med. Chem. 50 (2012) 441–448.
[18] F. Broccolo, G. Cainelli, G. Caltabiano, C.E.A. Cocuzza, C.G. Fortuna, P. Galletti, D. Giacomini, G. Musumarra, R. Musumeci, A. Quintavalla, J. Med. Chem. 49 (2006) 2804–2811.
[19] M. Baroni, G. Cruciani, S. Sciabola, F. Perruccio, J.S. Mason, J. Chem. Inf. Model. 47 (2007) 279–294.
[20] A. Pace, P. Pierro, Org. Biomol. Chem. 7 (2009) 4337–4348.
[21] S. Buscemi, A. Pace, R. Calabrese, N. Vivona, P. Metrangolo, Tetrahedron 57 (2001) 5865–5871.
[22] S. Buscemi, A. Pace, A. Palumbo Piccionello, I. Pibiri, N. Vivona, Heterocycles 63 (2004) 1619–1628.
[23] A. Palumbo Piccionello, A. Pace, I. Pibiri, S. Buscemi, N. Vivona, Tetrahedron 62 (2006) 8792–8797.
[24] A. Palumbo Piccionello, A. Pace, P. Pierro, I. Pibiri, S. Buscemi, N. Vivona, Tetrahedron 65 (2009) 119–127.
[25] K.C. Grega, M.R. Barbachyn, S.J. Brickner, S.A. Mizsak, J. Org. Chem. 60 (1995) 5255–5261.
[26] H. Biswajit Das, H. Sonali Rudra, A. Songita Songita, P. Mohammad Salman, H. Ashok Rattan, US Patent 2008/0188470, 2008.
[27] J.B. Locke, J. Finn, M. Hilgers, G. Morales, S. Rahawi, G.C. Kedar, J.J. Picazo, W. Im, K.J. Shaw, J.L. Stein, Antimicrob. Agents Chemother. 54 (2010) 5337–5343.
[28] O.A. Phillips, E.E. Udo, A.A. Ali, et al., Bioorg. Med. Chem. 35 (2003) 1156.
[29] M.B. Gravestock, D.G. Acton, M.J. Betts, M. Dennis, G. Hatter, et al. 13 (2003) 4179.
[30] L.M. Thomasco, E.A. Weaver, J.M. Ochoada, R.C. Gadwood, G.E. Zurenko, C.W. Ford, Abstr. Intersci. Conf. Antimicrob. Agents Chemother. Intersci. Conf. Antimicrob. Agents Chemother. 40 (2000) 216.
[31] S.-Y. Yhang, et al., Bioorg. Med. Chem. Lett. 14 (2004) 3881–3883.
[32] S.J. Brickner, Curr. Pharm. Des. 2 (1996) 175–194.
[33] C.H. Park, J. Med. Chem. 35 (1992) 1156–1165.
[34] M.R. Barbachyn, Adv. Exp. Med. Biol. 456 (1998) 219–238.
[35] S. Besier, A. Ludwig, J. Zander, V. Brade, T.A. Wichelhaus, Antimicrob. Agents Chemother. 52 (2008) 1570–1572.
[36] A. Liakopoulos, C. Neocleous, D. Klapsa, M. Kanellopoulou, I. Spiliopoulou, K.D. Mathiopoulos, E. Papafrangas, E. Petinaki, J. Antimicrob. Chemother. 64 (2009) 206–207.
[37] J.L. Hansen, P.B. Moore, T.A. Steitz, J. Mol. Biol. 330 (2003) 1061–1075.
[38] V. Meka, S.K. Pillai, G. Sakoulas, C. Wennersten, L. Venkataraman, P.C. DeGirolami, G.M. Eliopoulos, R.C. Moellering Jr., H.S. Gold, J. Infect. Dis. 190 (2004) 311–317.
[39] D.M. Livermore, M. Warner, S. Mushtaq, S. North, N. Woodford, Antimicrob. Agents Chemother. 51 (2007) 1112–1114.
[40] V.G. Meka, H.S. Gold, A. Cooke, L. Venkataraman, G.M. Eliopoulos, R.C. Moellering, S.G. Jenkins, J. Antimicrob. Chemother. 54 (2004) 818–820.
[41] J.B. Locke, M. Hilgers, K.J. Shaw, Antimicrob. Agents Chemother. 53 (2009) 5275–5278.
[42] F. Perruccio, J. Mason, S. Sciabola, M. Baroni, in: G. Cruciani (Ed.), Molecular Interaction Fields in Drug Discovery, Methods and Principles in Medicinal Chemistry, vol. 27, Wiley-VCH, Weinheim, 2005, pp. 83–102.
[43] S. Cross, M. Baroni, E. Carosati, P. Benedetti, S. Clementi, J. Chem. Inf. Model. 50 (2010) 1442–1450.
[44] P.J.A. Goodford, J. Med. Chem. 28 (1985) 849–857.
[45] E. Carosati, S. Sciabola, G. Cruciani, J. Med. Chem. 47 (2004) 5114–5125.
[46] The GRID Package, Version 22, is distributed from Molecular Discovery Ltd. http://www.moldiscovery.com.
[47] E. Carosati, G. Cruciani, A. Chiarini, R. Budriesi, P. Ioan, R. Spisani, D. Spinelli, B. Cosimelli, F. Fusi, M. Frosini, R. Matucci, F. Gasparrini, A. Ciogli, P.J. Stephens, F.J. Devlin, J. Med. Chem. 49 (2006) 5206–5216.
[48] E. Carosati, R. Mannhold, P. Wahl, J.B. Hansen, T. Fremming, I. Zamora, G. Cianchetta, M. Baroni, J. Med. Chem. 50 (2007) 2117–2126.
[49] R. Budriesi, B. Cosimelli, P. Ioan, M.P. Ugenti, E. Carosati, M. Frosini, F. Fusi, R. Spisani, S. Saponara, G. Cruciani, E. Novellino, D. Spinelli, A. Chiarini, J. Med. Chem. 52 (2009) 2352–2362.
[50] G. Muratore, L. Goracci, B. Mercorelli, A. Foeglein, P. Digard, G. Cruciani, G. Palù, A. Loregian, Proc. Natl. Acad. Sci. U. S. A. (2012), http://dx.doi.org/10.1073/pnas.1119817109. (Published ahead of print 02.04.12).
[51] S. Sciabola, R. Stanton, J.E. Mills, M.M. Flocco, M. Baroni, G. Cruciani, F. Perruccio, J.S. Mason, J. Chem. Inf. Model. 50 (2010) 155–169.
[52] S. Banala, R.D. Süssmuth, ChemBioChem 11 (2010) 1335.
[53] Clinical and Laboratory Standards Institute. Approved Standard, Methods for Dilution Antimicrobial Susceptibility Tests for Bacteria That Grow Aerobically, ninth ed., vol. 32, M07–A9, Wayne, Pennsylvania, 2011.
[54] E.C. Pirtle, Am. J. Vet. Res. 27 (1966) 747–749.
[55] D.P. Aden, A. Fogel, S. Plotkin, I. Damjanov, B.B. Knowles, Nature 282 (1979) 615–616.
[56] G. Pozzi, M. Guidi, F. Laudicina, M. Marazzi, L. Falcone, R. Betti, C. Crosti, E. Müller, G.E. Di Mattia, V. Locatelli, A. Torsello, J. Endocrinol. Invest. 27 (2004) 142–149.
[57] A. Bulbarelli, E. Lonati, E. Cazzaniga, M. Gregori, M. Masserini, Mol. Cell. Neurosci. 42 (2009) 75–80.
[58] D.A. Case, T.E. Cheatham, T. Darden, H. Gohlke, R. Luo, K.M. Merz, A. Onufriev, C. Simmerling, B. Wang, R.J. Woods, J. Comput. Chem. 26 (2005) 1668–1688.
[59] L.L.C. Schrodinger, The PyMOL Molecular Graphics System, Version 1.5r3 (2010).
[60] M. Rother, K. Rother, T. Puton, J.M. Bujnicki, Nucleic Acids Res. 39 (2011) 4007–4022.
[61] D.A. Case, T.A. Darden, T.E. Cheatham, C.L. Simmerling, J. Wang, R.E. Duke, R. Luo, M. Crowley, R.C. Walker, W. Zhang, K.M. Merz, B. Wang, S. Hayik, A. Roitberg, G. Seabra, I. Kolossvary, K.F. Wong, F. Paesani, J. Vanicek, X. Wu, S.R. Brozell, T. Steinbrecher, H. Gohlke, L. Yang, C. Tan, J. Mongan, V. Hornak, G. Cui, D.H. Mathews, M.G. Seetin, C. Sagui, V. Babin, P.A. Kollman, Amber 10, University of California, San Francisco, 2008.
[62] Chemical Computing Group, Inc, 2011.
[63] J. Wang, R.M. Wolf, J.W. Caldwell, P.A. Kollman, D.A. Case, J. Comput. Chem. 25 (2004) 1157–1174.
[64] J.P. Brincat, E. Carosati, S. Sabatini, G. Manfroni, A. Fravolini, J.L. Raygada, D. Patel, G.W. Kaatz, G. Cruciani, J. Med. Chem. 54 (2011) 354–365.